Norwegian University of Science and Technology.
Department of Petroleum Engineering and Applied Geophysics.

Master of Science Thesis:

ROCK PHYSICS DEPTH TREND ANALYSIS USING SEISMIC STACKING VELOCITY

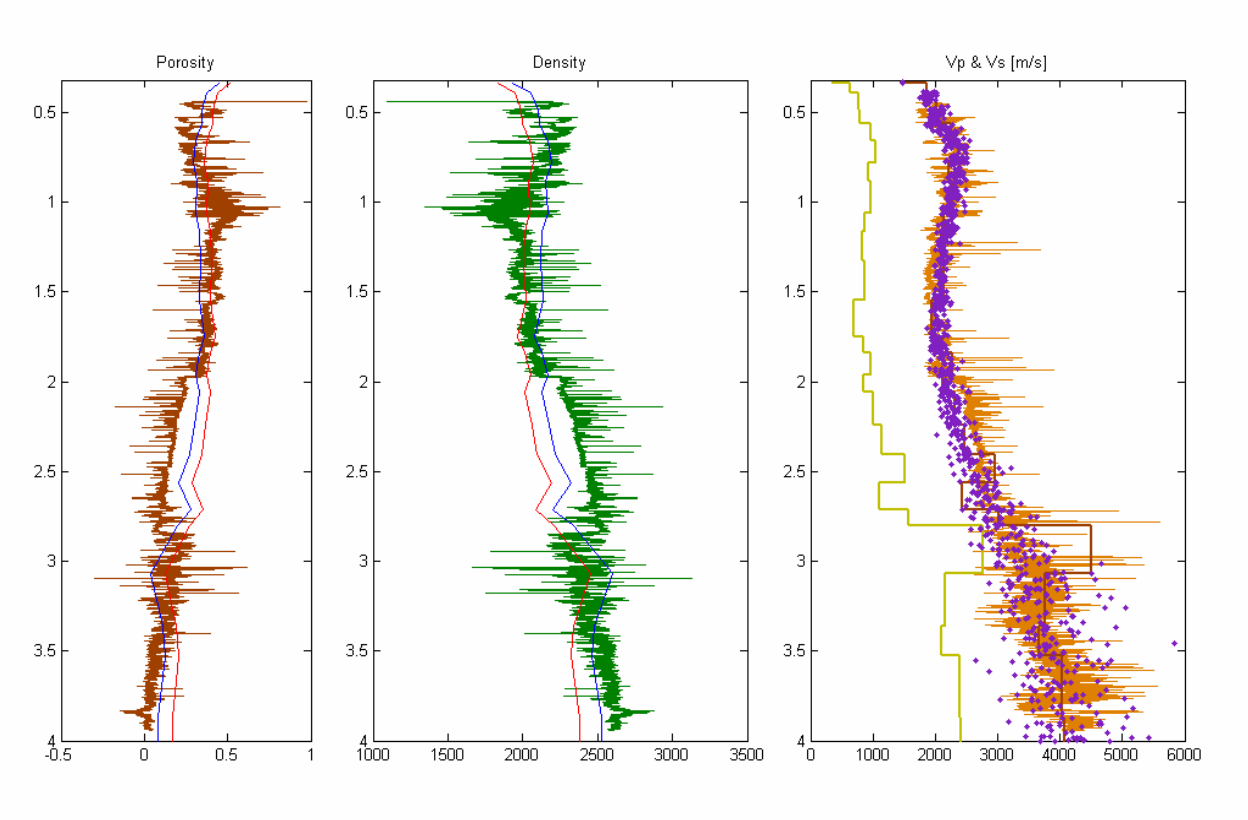

By: **Phuong Hoang**

Trondheim, Norway, June 2006.

NTNU

Norwegian University of Science and Technology

Faculty of Engineering and Technology

Department of Petroleum Engineering and Applied Geophysics

Study Programme in Earth Sciences and Petroleum Engineering.

MASTER OF SCIENCE THESIS

The candidate's name:	***Phuong Hoang.***
Supervisors:	***Bjørn Ursin (NTNU) and Per Avseth (Norsk Hydro).***
Title of Thesis:	***Rock physics depth trend analysis using seismic stacking velocity.***
Area of specialization:	***Petroleum Geosciences/Seismic.***
Time interval:	***January - June 2006.***

.....

Teacher

Abstract

Quantitative seismic interpretation is becoming more and more important in exploration and characterization of petroleum reservoirs. In this technology, rock physic analysis combined with seismic attributes has become a key strategy.

Nature creates inhomogeneous anisotropic rocks where the rock physics properties vary at different positions and directions. It is important to analyze and quantify the property changes as a function of depositional and burial trends in order to improve our detectability of petroleum reservoirs from seismic data.

In this thesis, we have presented a new methodology to obtain rock physics properties as a function of burial depth, i.e., rock physics depth trends (RPDTs), from well log and seismic data. To obtain RPDTs, several authors have suggested using rock physics models calibrated to well log data or constrained by diagenetic models. We present an alternative way to extract these from seismic stacking velocities. This is the main focus of the thesis.

We apply our methodology to extract RPDTs from seismic stacking velocities in the Njord Field area, located in the Norwegian Sea. We find that the seismic interval velocity trend matches nicely to the sonic velocity at the well location, especially above Base Cretaceous. By combining empirical RPDTs with seismic RPDTs, we are able to interpret and quantify the rock properties of different rock physics events that have occurred in Njord Field at well location and in the areas without well log information.

In this thesis we have successfully demonstrated how stacking velocities can be used to improve our understanding about normal mechanical compaction trends, tectonic activity and diagenetic events. This information is important for improved overburden and reservoir characterization, especially in areas with sparse or no well log data.

TABLE OF CONTENTS

INTRODUCTION

Seismic data has a vital play in exploration and characterization of petroleum reservoirs. The amount of easy-to-find reservoirs is decreasing rapidly while the need of oil and gas is increasing. We are facing difficulties in finding smaller, more subtle reservoirs with higher risks and costs. Qualitative seismic interpretation steps forward to become quantitative seismic interpretation. From seismic data, we do not simply need information about structural geometry and bulk rock volumes of potential reservoirs, but we also want to characterize their detailed properties, to quantify and to minimize risks. Rock physics analysis combined with seismic attributes has become a key strategy in quantitative seismic interpretation.

At big scales, rock physic properties are constrained by basin type, burial history and depositional environment. Nature created inhomogeneous anisotropic rocks where properties at different positions and directions are different. Lateral changes of rock properties are mostly related to depositional environment systems. Study of seismic lithofaces constrained by well data could help to quantify rock physics away from well locations. Vertically, rock properties are affected by the burial history, overburden, pressure, temperature, diagenetic events and subsidence rate. The study about the trends of rock physic properties as a function of depth is one of the key issues in rock physic analysis.

We can define a rock physics template (RPT) to account for various trends of rock physic properties in a depositional system. The terminology of RPT was introduced by Avseth et al. (2005) in the book Quantitative Seismic Interpretation. Rock physics depth trends (RPDT), are defined in a similar sense and describe the changes of rock properties in the vertical direction. In general, one can understand an RPDT as a trend in the depth direction of a particular rock physic property such as velocity, density and porosity. The study of RPDT is one of the main objectives of this diploma thesis.

To obtain RPDTs, we can use rock physics models calibrated to well log data (Avseth et al, 2005) or constrained by diagenetic models (Bremk, 2005; Droge, 2006). An alternative way to obtain RPDTs is to extract these from seismic stacking velocities. This is the main focus of this study. The different methods used to calculate RPDTs are presented in the first two chapters of the thesis.

Seismic RPDT calculation is introduced in the first chapter. The method focuses on calculating interval velocity from stacking velocity using DIX equation. Since we do not have

shear data, general transform equations are utilized to estimate Vs velocity and density depth trends from Vp depth trend.

The second chapter is about empirical RPDTs calculation. In this chapter, we discuss how to model RPDTs of porosity, velocity, density, pressure and other depth trends for different lithologies in different rock physics scenarios such as uplifting-erosion, mechanical compaction, overpressure and chemical compaction.

The third chapter is to calculate RPDTs for Njord field data, Norwegian Sea. First, we will interpret given seismic, velocity and well log data to obtain basic understanding of the subsurface structure and rock physics scenarios related to local burial history. Interpretation results will be used as regional information for modelling of empirical RPDTs afterwards. Our main interest is to reveal abnormal rock physics intervals where well log data deviate from the normal mechanical compaction RPDTs. We will try to interpret and quantify these anomalies by using well data and RPDTs.

The workflow and main purposes in chapter three can be summarized below:

- ✓ Model empirical RPDTs for normal mechanical compacted rock in Njord field. Combine modelled depth trends with well log data to interpret abnormal rock physic scenarios occurred during burial history.
- ✓ Model possible abnormal rock physics scenarios occurred in Njord field. Using well log and laboratory data if available to quantify rock properties for each abnormal rock physic scenario.
- ✓ Calculate interval velocity from stacking velocity in Njord field. We expect that with high quality stacking velocity and right method used, the calculated seismic interval velocity will match well to Sonic logging data. This means that we can replace well velocity by seismic interval velocity to interpret rock physics scenarios and also possible to quantify the rock properties in the area without well data.
- ✓ Calculate seismic interval velocity for locations away from the wells. Combine empirical and seismic RPDTs to analyze rock physic scenarios and if possible try to quantify rock property parameters.

Chapter 1

SEISMIC ROCK PHYSICS DEPTH TRENDS

1.1. Introduction.

In order to calculate the RPDT, we need to have interval velocity–depth functions from seismic data. The methods used to calculate interval velocity and delineate reflector geometry in depth are shown in Table 1.

Layer velocity	***Reflector Geometry***
Dix conversion of rms velocity	Vertical ray time to depth conversion (Vertical stretch)
Stacking velocity inversion	Image ray time to depth conversion (Map migration)
Coherency inversion	Post stack depth migration
Image gather analysis	Prestack depth migration

Table 1. Interval velocity calculation and reflector geometry delineation methods.

The choice of methods to be used is depended on the complexity of subsurface structure and the variation of velocity in layers. With horizontal reflector geometry and no lateral velocity variation, a combination of Dix conversion or stacking velocity inversion and vertical ray time to depth may give a good result. However in complex structures, image gather and prestack depth migration is the best combination. Analysed models can be updated by semblance residual analysis or reflection tomography technique.

To simplify, we assume the subsurface composes horizontal layers with mild lateral variation in velocity. The procedure using Dix conversion method to calculate interval velocity and then depth trends can be summarized in the flow chart 1.

From seismic processing, we have final stacked seismic data and stacking velocity. Commonly we do not have shear wave data but only compressional wave stacking velocity cube (Vp).

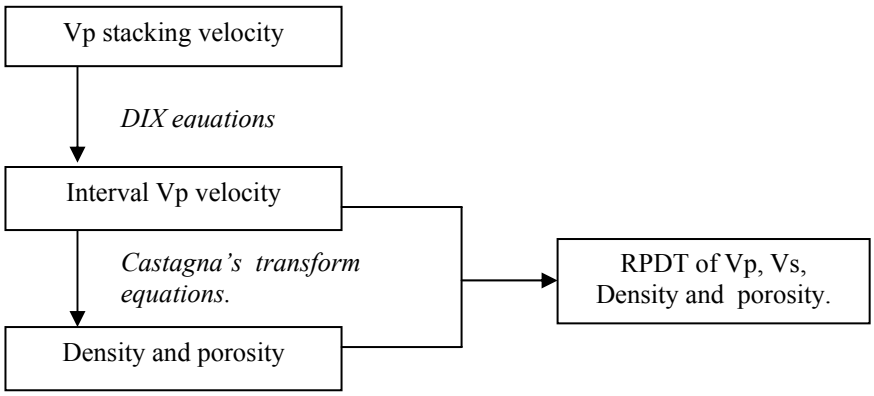

Chart 1. Rock physic depth trend calculation by Dix conversion method

Basically, stacking velocity is the velocity that gives best-stacked sections. Depending on subsurface structure complexity and our need, velocity analysis can be done in time or in depth domain together with post-stack or pre-stack migration residual velocity analysis. In general, the accuracy of velocity analysis is higher if we use pre-stack migration technique in depth domain. In time domain, we assume that subsurface lithology boundaries are horizontal and P waves have small spread stacking velocity that is similar to root mean squared velocity (rms) which is defined as:

$$V_{rms}^2 = \frac{1}{T_o}\sum_{i=1}^{N} V_i^2 \Delta\tau_i \ , \qquad (1)$$

where V_i and $\Delta\tau_i$ are interval velocity and vertical two way travel time in the ith layer respectively. A layer can be understood as the interval between two picks in velocity spectrum.

Knowing the two way traveltime and stacking velocity at each velocity pick, we can calculate interval velocity by using the well known Dix equation:

$$V_{int\,i} = \sqrt{\frac{V_{rmsi}^2\tau_i - V_{rmsi-1}^2\tau_{i-1}}{\tau_i - \tau_{i-1}}} \qquad (2)$$

where V_{inti} is interval velocity in the ith layer and τ_i is zero offset two way time from top of 1st layer to the top of layer i.

Without shear wave data, estimation of V_s from compressional wave reflection data at far offsets is a complex procedure. The easier way is using empirical V_p-V_s relation studied in the area. We do the same to get a V_p versus density (ρ) relation. After having V_p, V_s and ρ we can easily create the depth trend for acoustic impedance (AI) and elastic impedance (EI).

1.2. Travel time function and stacking velocity.

In a horizontally stratified earth composed of horizontal isovelocity layers, M. Taner and Koehler (1969) derived the traveltime equation of reflected P wave (PP) waves going down from a source, reflected at top of layer n^{th} and go back to a receiver can be expressed as:

$$T^2 = C_0 + C_1 X^2 + C_2 X^4 + C_3 X^6 + ... \tag{3}$$

where $C_0 = T_0^2$ and $C_1 = 1/V_{rms}^2$, and C_2, C_3 … are complicated functions. There are several authors have suggested approximate travel time as a function offset X in different media. For example Stovas and Ursin (2005) introduced an approximation for an isotropic constant velocity gradient medium as:

$$T^2 = T_0^2 + \frac{1}{V_{NMO}^2} X^2 - \frac{S-1}{4V_{NMO}^4 \left(T_0^2 + \frac{S-1}{2} \frac{X^2}{V_{NMO}^2} \right)} X^4 \tag{4}$$

where S is the heterogeneity factor and V_{NMO} is equal to V_{rms}.

Alkhalifah and Tsvankin (1995) introduced traveltime approximation for a laterally homogeneous anisotropic medium as:

$$T^2 \cong T_0^2 + \frac{1}{V_{PNMO}^2} X^2 - 2\eta \frac{1}{T_0^2 V_{PNMO}^4 \left[1 + (1+2\eta) \frac{X^2}{T_0^2 V_{PNMO}^2} \right]} X^4 \tag{5}$$

where $\eta = (\varepsilon - \delta)/(1+2\delta)$ is a combination of Thomsen anisotropy parameters.

In conventional seismic processing and also in this study, we assume small spreading (offsets are small compared to depth) to simplify equation (3) into:

$$T^2 = T_0^2 + \frac{1}{V_{rms}^2} X^2 \tag{6}$$

In this special case, the stacking velocity is as same as rms velocity.

We have assumed subsurface structure composed of isotropic and horizontal layers. What if the structure is complex and anisotropic? In order to solve the anisotropy problem we must include the higher order of X in equation (3) during processing. However, to do this we need interpretation about the layer's properties, i.e. Thomsen's anisotropy parameters which are related to rock physic analysis. This work is far beyond consideration of conventional

seismic processing. Hence, anisotropic velocity caused by complexity of subsurface structure problem can be solved by dip move out (DMO) and migration techniques. When subsurface structure is very complex and there is strong lateral variation of velocity, pre-stacking depth migration will give the best stacking velocity. Details of velocity analysis and further discussion can be found in Yilmaz (2001).

1.3. Seismic rock physics depth trends.

1.3.1. Seismic Vp depth trend.

The rms velocity is important to seismic processing but not in rock physic analysis. Interval velocity is the average velocity in a particular interval. If the rock interval is isotropic or less homogeneous, seismic interval velocity calculated from stacking velocity is considered as real rock parameters. In this case, we can use interval velocity for rock physic analysis.

In the time domain, the procedure to calculate interval velocity from stacking velocity is as folows:

i. Extract the rms and travel time at each velocity point.
ii. Use equation (2) to calculate interval velocity.
iii. Use interval velocity and travel time to convert time to depth.

Schematically, we can explain the procedure to calculate Vp interval velocity from stacking velocity by using Dix conversion method as in Figure 1.

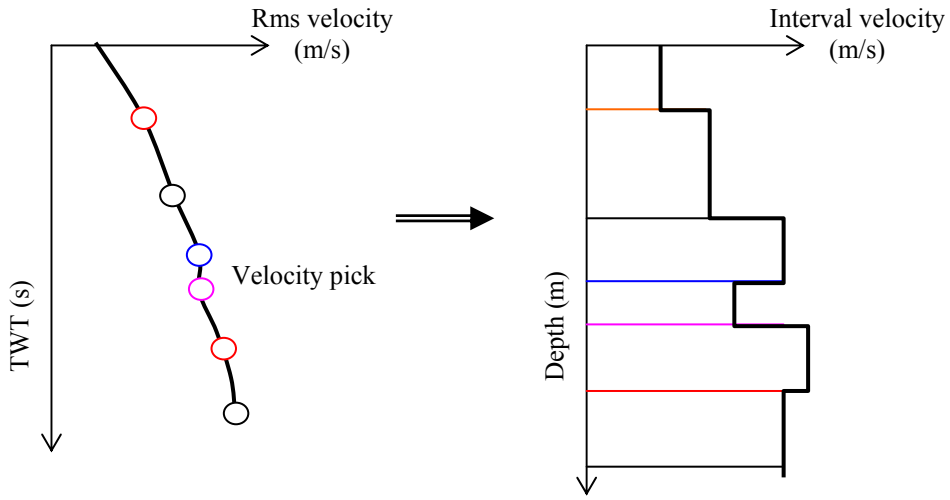

Figure 1. Vp interval velocity depth trend calculated from rms velocity

1.3.2. Vs depth trend.

If we have shear data, we will use the same method as we did for Vp to get shear wave interval velocity depth trend. However, normally we do not have Vs rms data so that we have to use an empirical relation to calculate a corresponding Castagna et al. (1993) interval Vs depth trend. Below are some examples of empirical and linear Vp-Vs relationships from Castagna et al. (1993):

Limestones:

$$V_S = -0.055V_P^2 + 1.0168V_P - 1.0305 \quad \text{(km/s)} \tag{7}$$

Dolomites:

$$V_S = 0.5832V_P - 0.0777 \quad \text{(km/s)} \tag{8}$$

Sandstones and shale with saturated water:

$$V_S = 0.8042V_P - 0.8559 \quad \text{(km/s)} \tag{9}$$

In this study, equation 9 is used to calculate Vs velocity. We have noted that these relations are applicable to some specific area but not globally valid. To have a precise Vs depth trend derived from Vp, empirical relations should be calibrated with the well data in the studied area.

1.3.3. Porosity, density and other RPDTs.

Porosity:

Ramm and Bjørlykke (1994) suggested a clay-dependent exponentional regression model for porosity versus depth of sands, valid only for mechanical compaction:

$$\phi = Ae^{-(\alpha+\beta C_I)Z} \tag{10}$$

where A, α and β are regression coefficients. Coefficient A is related to the initial porosity at zero burial depth. α is a framework grain stability factor. β is a factor describing the sensitivity towards increasing clay index (C_I). Clay index is defined by the volume of clay relative to the total volume of stable framework grain (Qz).

Porosity for different lithologies can be calculated directly from density using the following equation:

$$\phi_{density} = \frac{\rho_{ma} - \rho_{measured}}{\rho_{ma} - \rho_{fluid}} \tag{11}$$

where matrix density is assumed to be 2.65 (kg/m^3) for sandstone, 2.660 for shale, 2.680 for mudstone and fluid density is 1.05 (kg/m^3). These values can be adjusted for different locations.

Density:

The relation of porosity and density is given by:

$$\rho_b = \phi\rho_{fl} + (1-\phi)\rho_{min} \tag{12}$$

where ρ_b is the total density, ρ_{fl} is the fluid density and ρ_{min} is the mineral density.

Additionally, one can use the velocity-density transforms (gm/cm^3 and ft/s) for different lithologies proposed by Castagna (1993) below:

Sand: $\rho = 0.200\ V_P^{0.261}$

Shale: $\rho = 0.204\ V_P^{0.265}$ (13)

Acoustic impedance:

Having Vp, Vs, density trends, we can calculate acoustic impedance (AI) by using the formula:

$$AI = V_P\rho_b \tag{14}$$

Velocity ratio of Vp and Vs is another important parameter for lithologies discrimination in rock physic analysis.

Chapter 2

EMPIRICAL ROCK PHYSICS DEPTH TRENDS

2.1. Introduction.

In order to model empirical RDPTs, it is important to understand the processes and factors affecting rock physics properties. During accumulating, sedimentary factors like sorting, grain size, clay content, grain shape, mineralogy and packing will affect the rock physics properties of sediments. During burial, the sediments will be compacted both mechanically and chemically i.e. diagenesis. This is related to both pressure and temperature increase. Eventually the sediments become rock. Rock tends to be more compacted and harder with depth. Porosity and permeability reduce while velocities increase.

In this chapter, we focus our study on the effects of diagenetic processes on rock properties after deposition. With regards to chapter three, we limit our consideration to diagenetic processes that have occurred in Njord field, Norwegian Sea region. Empirical RPDTs are modelled for main rock physic scenarios include mechanical compaction (eogenesis); cementation and overpressure (mesogenesis) and uplift-erosion (telogenesis).

We are not going to model all rock physic properties but limit ourselves to porosity, density, effective pressure and velocity. These rock physic properties are not stand-alone parameters. They are linked to each other. We can infer to their relations from the well-known equations below:

$$V_P = \sqrt{\frac{K_{sat} + 4/3\mu_{sat}}{\rho}} \tag{12}$$

$$V_S = \sqrt{\frac{\mu_{sat}}{\rho}} \tag{13}$$

where K is saturated bulk rock modulus, μ is saturated shear modulus and ρ is density. Density varies with depths and can be calculated directly from porosity. Rock moduli K_{sat} and μ_{sat} vary with depth as a function of dry rock moduli (K_{dry} and μ_{dry}), fluid moduli (K_{fl}), porosity and effective pressure.

The workflow to model empirical RPDTs for a particular rock physics scenario include:

- ✓ Understand the diagenetic mechanism.

- ✓ Model porosity trend.
- ✓ Model dry rock and saturated rock moduli.
- ✓ Calculate velocity and other RPDTs.

We are able to model empirical RPDTs for a certain rock physic scenario in an area. However, it is important to note that we could not include all the possible diagenesis processes into one model. Models are normally simplified and local. Before applying them to an area we should check the validity of all assumptions.

2.2. Modelling of empirical RDPTs in different rock physic scenarios.

In the Norwegian Sea region, especially in Njord field, mechanical compaction, overpressure and cementation are found to be the important diagenetic processes, which have big impacts on porosity reduction. Uplifting and erosion events create discontinuities in rock density, porosity and moduli depth trends. Tectonic processes are also important to include in the modelling of rock physic depth trends.

First of all, we recall some basic knowledge about diagenesis. As introduced by Choquette and Pray (1970) and developed by Worden and Burley (2003), diagenesis is classified into eogenesis (early diagenesis), mesogenesis (burial diagenesis) and telogenesis (uplift and erosion after burial diagenesis).

Early diagenesis occurs in the shallow depths of several hundred meters. It is controlled by the depositional environment i.e. provenance, sediment component, sediment accumulating rate, meteoric water, climate, organic matter content. Although this process occurs at shallow depth and is not of our main interest target, its products will affect the later diagenesis.

Mesogenesis occurs after deposition and during burial to the depth of some kilometers. Mesogenesis is controlled by three important factors, which are pressure, temperature and fluid composition. Generally it is divided into mechanical compaction, chemical compaction and pressure solution. Mechanical compaction processes may include grain rearrangement, deformation/bending and dissolution. Chemical compaction relates to the changes in mineral chemistry and chemical reactions. The chemical compaction processes could be cementation (Quartz, carbonate), illite-forming reactions, grain coating processes of clay minerals and organic matters. Pressure solution is important in carbonate rock and in Quartz-rich sandstones. Stylolites created by this mechanism will enhance porosity.

Telogenesis occurs in areas of uplifting. Due to tectonic events or differential compaction, rock formations are uplifted and exposed to the air. Weathering and physical processes will erode exposed rock.

2.2.1. Mechanical compaction.

During burial, overburden is getting thicker, overburden pressure increases and thus underlying rocks become harder. Mechanical compaction is controlled mainly by pressure regime. This process may include grain rearrangement, deformation/bending and mineral dissolution/replacement. Different lithologies, i.e. sand and shale, have different behaviours to mechanical compaction.

Grain rearrangement is the process in which grains rearrange them to have a more stable and packing texture. For example, a mixture of un-oriented shale particles will become laminated while sand grains will change from cubic to rhombic texture as in Figure 2a. Grain rearrangement is the main process, which dramatically reduces porosity of rock.

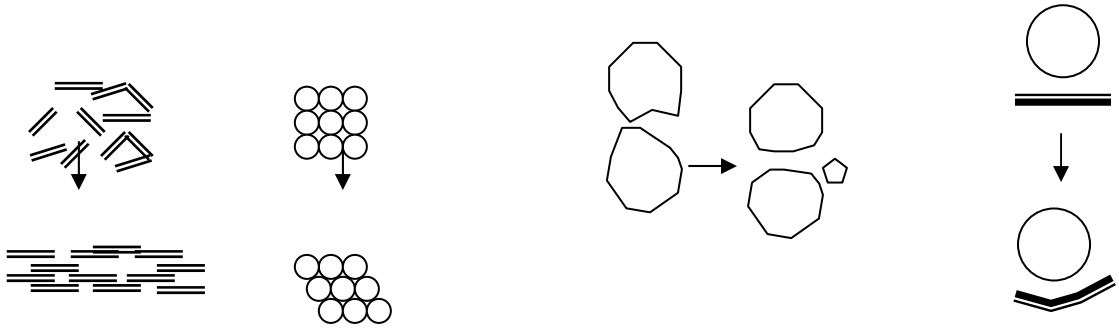

Figure 2: Shale and sand rearrangement (a); rock fragment deformation (b) and bending (c).

Rock deformation and bending: poorly rounded grains will become more rounded. Sharp edges under mechanical compaction will be crushed out and destroyed; contact surface's area between grains hence increases. Small particles from broken edges will fill up the pore space and reduce the porosity (Figure 2b). Laminated elongate material such as muscovite, biotite are easily blended (Figure 2c). Differential mechanical compaction can also create micro fractures. This process is particularly important in carbonate rock.

Mechanical compaction reduces porosities of shale and sand. Schematically, we can compare the porosity changes in shale and sand as in Figure 3. Stage 1 is during sediment deposition, stage 2 is during burial and stage 3 in sand is cementation while in shale, fluid is being squeezed out.

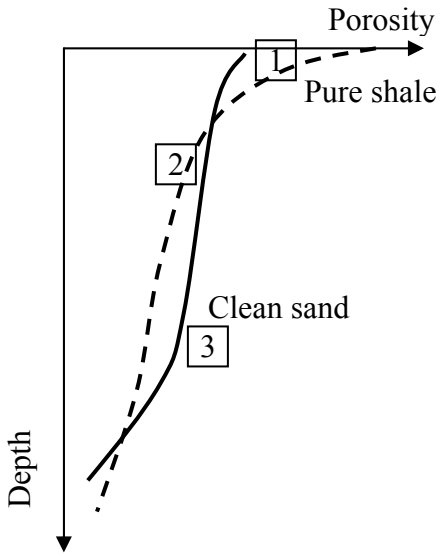

Figure 3: Shale and sand porosity depth trends (schematic).

Empirical porosity depth trend.

As mentioned in the previous section, in the Norwegian Sea region we use Ramm and Bjørlykke empirical model to calculate porosity functions, which is valid only for mechanical compaction. This model works very well in the Norwegian Sea where the mechanical compaction dominates the mesogenetic processes from surface to the depth of 2.5-3 km (Ramm et al., 1992). In the area where chemical compaction occurred, this model is probably not applicable.

Let us recall the equation 10:

$$\phi = Ae^{-(\alpha+\beta C_I)Z}$$

where A, α and β are regression coefficients. Coefficient A is related to the initial porosity at zero burial depth. α is a framework grain stability factor. β is a factor describing the sensitivity towards increasing clay index (C_I). Clay index is defined by the volume of clay relative to the total volume of stable framework grains.

Based on this equation, we can establish the porosity depth trend for predefined lithologies. The following example is from the Glitne field in North Sea. After calibrating equation 10 to well log data, we have two porosity exponential functions for clean sand in Heimdal formation and clean shale in Lista formation as below:

$$\phi = 45e^{-(0.10+0.27x0.1)Z} \tag{14}$$

$$\phi = 60e^{-(0.10+0.27x2.0)Z} \tag{15}$$

Figure 4 shows the porosity depth trends of pure shale and clean sand. Pure shale has initial porosity of 60% while clean sand has 45%.

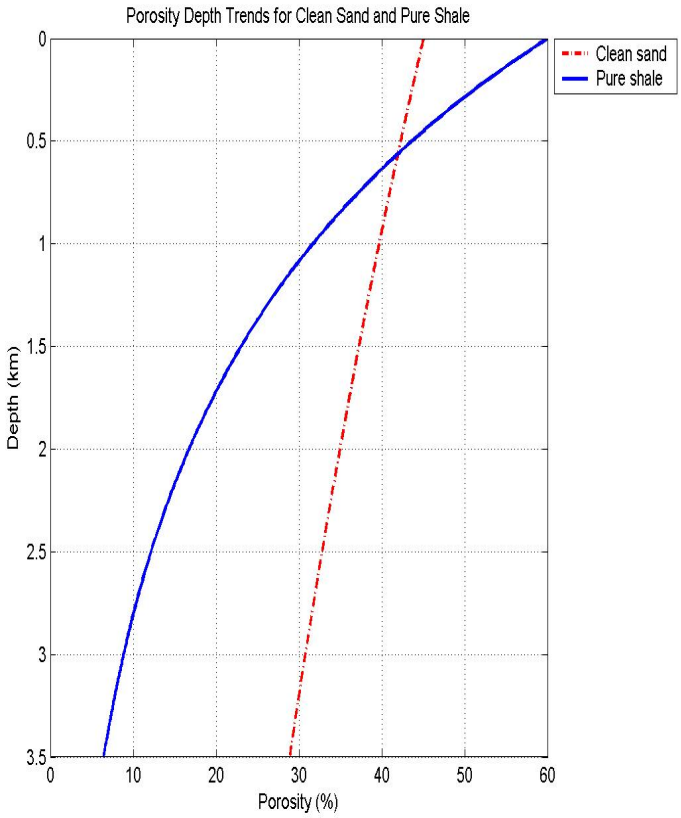

Figure 4. Pure shale porosity depth trend in Lista formation and clean sand porosity depth trend in Heimdal formation, Norwegian Sea.

Empirical rock moduli depth trends.

As proposed by Avseth et al., (2005) Hertz-Mindlin theoretical equations are used to calculate dry rock moduli (K_{dry} and μ_{dry}) of unconsolidated sediment as a function of porosity and effective pressure:

$$K_{HM} = \left[\frac{n^2 (1-\phi)^2 \mu^2}{18\pi^2 (1-v)^2} P_{eff} \right]^{\frac{1}{3}} \tag{16}$$

$$\mu_{HM} = \frac{5-4v}{5(2-v)} \left[\frac{3n^2 (1-\phi)^2 \mu^2}{2\pi^2 (1-v)^2} P_{eff} \right]^{\frac{1}{3}} \tag{17}$$

where K_{HM} (or K_{dry})and μ_{HM} (or μ_{dry}) are the dry rock bulk and shear moduli respectively; P_{eff} is the effective pressure; μ and v are the shear modulus and Poission's ratio of the solid phase and n is the coordinate number (the average number of contacts per grain).

The Poisson's ratio can be expressed as:

$$v = \frac{3K_{HM} - 2\mu_{HM}}{2(3K_{HM} + \mu_{HM})} \tag{18}$$

Effective pressure is the different pressure between the overburden lithology pressure (confining pressure, P_c) and the pore fluid pressure (P_f). Among others, Prasad and Manghnani (1997) applied the following formulation:

$$P_{eff} = P_c - mP_f \tag{19}$$

where m is effective stress coefficient.

From the density log, we can calculate confining pressure by integral function:

$$P_c = g \int_0^Z \rho_b(z) dz \tag{20}$$

where g is the acceleration of gravity, $\rho_b(z)$ is bulk density at depth z.

Assuming that from depth 0 to Z, pores are connected together and connected to open surface, we can calculate pore fluid as the hydrostatic pressure by equation:

$$P_f = g \int_0^Z \rho_f(z) dz \tag{21}$$

Carcione et al., (2001) introduced a method to estimate pore pressure from seismic reflection data. They used high-resolution velocity analyzed by tomoghraphy technique in depth domain to estimate *m* coefficient. The method has been applied to real data and had good results. However, in the limited time, we are not going to use this method. Instead, we simplify equation 19 by assigning static measurement to $m \approx 1$ (Zimmerman et al., 1986). Equation 19 becomes:

$$P_{eff} = g\int_0^Z \left(\rho_b(z) - \rho_f(z)\right)dz \tag{22}$$

Coordination number *n* can be calculated by empirical equation introduced by Murphy (1982):

$$n = 20 - 34\phi + 14\phi^2 \tag{23}$$

Previously, we have modelled the porosity depth trend, so that we can calculate the coordination number. Combining porosity, effective pressure and coordination number as functions of depth, we can calculate dry rock moduli using equations 16 and 17.

Empirical velocity depth trend.

In the presence of fluid, V_p velocity is calculated by using Gassmann's equation:

$$\rho V_P = K_{dry} + \frac{4}{3}\mu_{dry} + \frac{\left(1 - K_{dry}/K_{ma}\right)^2}{\frac{\left(1 - \phi - K_{dry}/K_{ma}\right)}{K_{ma}} + \frac{\phi}{K_{fl}}} \tag{24}$$

Dry rock Fluid

where

ρ : Rock density,

K_{dry}: Dry rock bulk modulus,

μ_{dry}: Dry rock shear modulus

K_{ma}: Matrix bulk modulus,

K_{fl}: Fluid bulk modulus,

ϕ: Rock porosity.

Six inputs are needed to calculate velocity. We have calculated dry rock bulk and shear moduli. The porosity is also modelled. Density is calculated directly through porosity by using following equation:

$$\rho = \rho_{fl}\phi + \rho_{ma}(1-\phi) \tag{25}$$

where ρ_{ma} is density of matrix i.e. minerals, if the rock is composed by more than one mineral, averaged mineral density is taken; ρ_{fl} is fluid density. If fluid contains brine water, oil and gas, its density is calculated by equation:

$$\rho_{fl} = \rho_{BR}S_{BR} + \rho_{oil}S_{oil} + \rho_{gas}S_{gas} \tag{26}$$

where S is saturation in percentage.

If well log is available, we will have enough information about fluid properties to calculate total density. If not we can assume that the formation is composed by one mineral i.e. quartz or clay and pore spaces are saturated with brine water. Taking the known experimental values we can calculate rock density ρ using equation 25.

Matrix bulk modulus (K_{ma}) can be estimated by using Voigt-Ruess-Hill mixing models. Voigt introduced upper bound of rock moduli (K_V), Ruess introduced lower bound of rock moduli (K_R) and Hill averaged upper and lower moduli to get effective (K_{ma}) as in equations 27, 28, 29, respectively.

$$\frac{1}{K_R} = \frac{N_1}{K_1} + \frac{N_2}{K_2} + \ldots + \frac{N_n}{K_n} \tag{27}$$

$$K_V = N_1K_1 + N_2K_2 + \ldots + N_nK_n \tag{28}$$

$$K_{ma} = (K_R + K_V)/2 \tag{29}$$

K_{fl} is estimated by using Voigt model if water and hydrocarbon is mixed in a uniform pattern. If fluid is mixed in patchy pattern, K_{fl} is calculated by using Ruess model.

There is a commonly used method to estimate K_{dry} by using equation:

$$K_{dry} = (1-B)K_{ma} \tag{30}$$

where B is Biot coefficient.

Biot coefficient is estimated by using empirical relation with porosity. There are several empirical relations proposed. For example, Krief et al., (1990) used relation:

$$B = 1 - [1 - \phi]^{\frac{3}{1-\phi}}$$

μ_{dry} can be calculated using equation:

$$\frac{K_{dry}}{\mu_{dry}} = \frac{2(\sigma_{dry} + 1)}{3 - 6\sigma_{dry}}$$

where σ_{dry} is Poisson's ratio can be estimated empirically for example σ_{dry} =0.125.

Instead of using equation 24, we can use the equation 12 to calculate Vp. The relation between dry rock moduli and saturated rock moduli is expressed as below:

$$K_{sat} = K_{ma} \frac{D}{1 + D}$$

$$D = \frac{K_{dry}}{K_{ma} - K_{dry}} + \frac{K_{fl}}{\phi(K_{ma} - K_{fl})}$$

$$\mu_{sat} = \mu_{dry}$$

2.2.2. Cementation.

Cementation is one of the processes of chemical compaction where, in preferable condition, precipitated material starts to form crystals and fill in pore spaces. Cementation initiation depends on the concentration of ions in pore fluid. When anions and cations of a certain mineral get saturated, cementation will occur. Common cements could be quartz, calcite cementation, carbonate cement (limestone and dolomite). Clay coating can be considered as a type of cementation. Chlorite coating to grains can prevent other types of cementation like quartz cementation. Figure 5 shows a model of quartz cementation over grows original quartz grains.

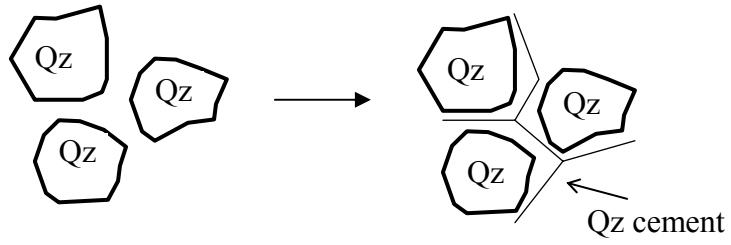

Figure 5: Quartz over growth cementation.

Empirical porosity depth trends.

Cementation reduces porosity, strengthens the rock and increases velocity. We need to know the cement volume as an important input to model porosity depth trend. In Norwegian Sea, one may use the following empirical porosity depth trend proposed by Ramm and Bjørlykke (1994).

$$\phi = \phi_D - k(Z - Z_D) \tag{16}$$

where ϕ_D is the porosity at depth Z_D where the cementation initiates. The constant k is the rate at which the cement volume increases with depth.

For example, in Glitne field in the North Sea, cementation is found to initiate at 2.2 km, whereas porosity for clean sands at that depth is 30%. After calibrating to well data, we have the coefficient k in the Glitne area equal to 13. Hence, the empirical porosity depth trend accounting for the effect of quartz cementation is:

$$\phi = 30 - 13(Z - 2.2)$$

Empirical rock moduli depth trend.

It is proposed by Avseth et al. (2005), that in the scenario of cementation in the North Sea, we use the contact-cement model, which was introduced by Dvorkin et al., (1994) to calculate dry rock moduli.

$$K_{dry} = n(1-\phi_c)M_c S_n / 6 \tag{31}$$

$$\mu_{dry} = 3K_{dry} / 5 + 3n(1-\phi_c)\mu_c S_\tau / 20 \tag{32}$$

where ϕ_c is critical porosity; K_s and μ_s are the bulk and the shear moduli of grain material, respectively; K_c and μ_c are the bulk and the shear moduli of the cement material, respectively; $M_c = K_c + 4\mu_c/3$ is the compressional modulus of the cement; and n is the coordinate number. The variables S_n and S_τ are:

$$S_n = A_n(\Lambda_n)\alpha^2 + B_n(\Lambda_n)\alpha + C_n(\Lambda_n)$$

$$A_n(\Lambda_n) = -0.024153\Lambda_n^{-1.3646}$$

$$B_n(\Lambda_n) = 0.2040\Lambda_n^{-0.89008}$$

$$C_n(\Lambda_n) = 0.00024649\Lambda_n^{-1.9864}$$

$$\Lambda_n = \frac{2\mu_c(1-\nu_s)(1-\nu_c)}{\pi\mu_s(1-2\nu_c)}$$

$$S_\tau = A_\tau(\Lambda_\tau, v_s)\alpha^2 + B_\tau(\Lambda_\tau, v_s)\alpha + C_\tau(\Lambda_\tau, v_s)$$

$$A_\tau(\Lambda_\tau, v_s) = -10^{-2}\left(2.26v_s^2 + 2.07v_s + 2.3\right)\Lambda_\tau^{0.079v_s^2+0.17v_s-1.342}$$

$$B_\tau(\Lambda_\tau, v_s) = \left(0.057v_s^2 + 0.093v_s + 0.202\right)\Lambda_\tau^{0.0274v_s^2+0.0529v_s-0.8765}$$

$$C_\tau(\Lambda_\tau, v_s) = 10^{-4}\left(9.654v_s^2 + 4.945v_s + 3.1\right)\Lambda_\tau^{0.01867v_s^2+0.401v_s-1.8186}$$

$$\Lambda_\tau = \frac{\mu_c}{\pi\mu_s}$$

$$\alpha = \left(\frac{2}{3}\frac{\phi_c - \phi}{1-\phi_c}\right)^{0.5}$$

$$v_c = 0.5\frac{K_c/\mu_c - 2/3}{K_c/\mu_c + 1/3}$$

$$v_s = 0.5\frac{K_s/\mu_s - 2/3}{K_s/\mu_s + 1/3}$$

Since porosity is a function of depth, using equation 31, 32 we can predict rock moduli in depth direction.

Empirical velocity depth trends.

Having porosity and dry rock moduli depth trends, we use the same method to get velocity depth trends as in mechanical compaction mechanism.

2.2.3. Uplifting and erosion.

Uplifting is normally caused by regional tectonic activities such as magmatic convection current, plate convergence and subsidence. Locally, it can be caused by differential compaction or salt dome development. In the uplifting area, subsurface formation is pushed up and exposed to the air. Weathering and physical processes occuring at the same time with uplifting activities will erode the exposed rock, ideally to the sea water level. When the uplifting ends, young sediment will fill up the eroded surface to create an unconformity. A simple uplifting and erosion process is illustrated in Figure 6.

The contrast between young and old rocks at the unconformity in terms of age, maturity and consolidation is depended on how much original stratigraphy was eroded and the current depth of the unconformity. When the contrast is high, we normally recognise strong positive reflection events in seismic data. During subsidence stage, young sediment is accumulated and become compacted; the contrast at the unconformity surface will be less. When the overlying rock becomes consolidated, it may be difficult to recognise the unconformity event based on rock physics depth trends.

Let assume that before uplifting sediment is at depth Z_1; during uplifting, this sediment was pushed up and eroded to depth 0; new sediment fills in and buries the original sediment to depth Z_2 (Figure 6).

Empirical porosity depth trend.

To model the porosity depth trend, we assume that during moving upwards from depth Z_1 to depth 0 and being buried down to the depth Z_1 again, the original rock does not change its properties. This assumption implies that there is no telogenetic process occurring when the rock is exposed to the air. For consolidated sand and shale this assumption might be reasonable but for carbonate rock, which is very sensitive to the change in meteoric water, this assumption may be not applicable.

Another assumption is that mechanical compaction is the only dominant mesogenetic process before and after uplifting. Mechanical compaction mechanism is also assumed to be the same so porosity depth trends of the same rock type before and after uplifting are similar. In relation to the processes in Figure 6, porosity depth trends modelled empirically by using Ramm and Bjørlykke theory are shown in Figure 7.

When Z_2 is less than Z_1 there is a sharp jump in the porosity at Z_2. The difference is $\phi_2 - \phi_1$. The difference is 0 when Z_2 is equal to Z_1. When Z_2 is greater than Z_1, the old/original rock and the young rock undergo mechanical compaction together; the porosity depth trend is as same as the one before uplifting.

When Z_2 is equal or greater than Z_1, the porosity follow the normal mechanical compaction porosity trend.

In summary, we assume discontinuous mechanical compaction to model the porosity depth trend in case of uplifting and erosion using Ramm and Bjørlykke theory. The input information we need is the current depth of unconformity and the thickness of eroded rock.

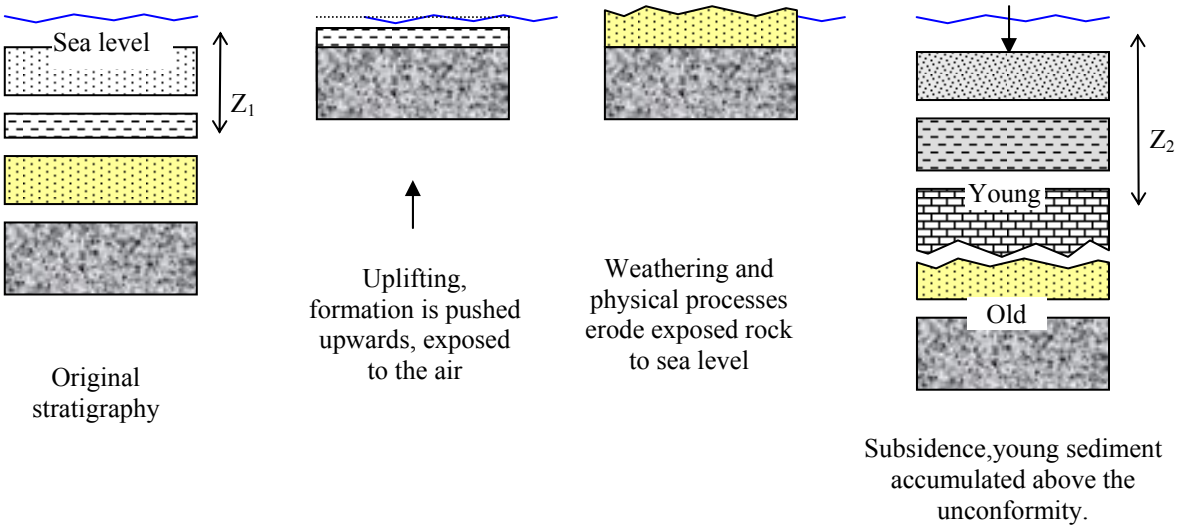

Figure 6: Uplifting and erosion process.

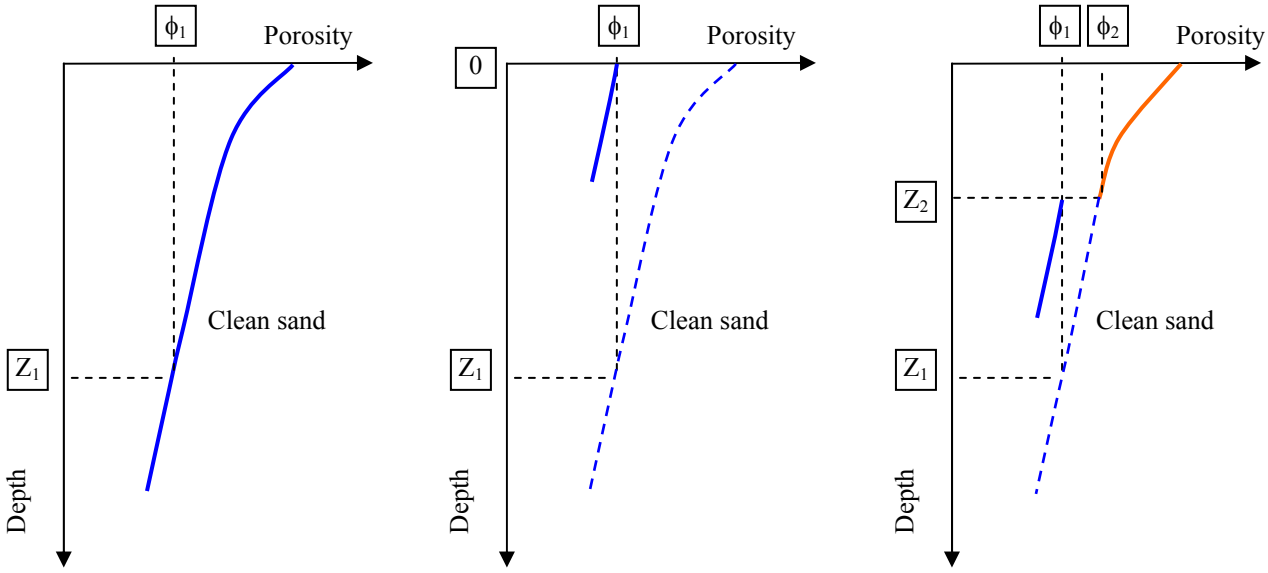

Figure 7: Porosity depth trend at depth Z_1 before uplifting, at depth 0 after erosion and depth Z_2 after new sediment filled in.

Other rock physic depth trends.

The other RPDTs are modelled as in the mechanical compaction part discussed in the section 2.2.1

Chapter 3

ROCK PHYSICS DEPTH TRENDS IN NJORD FIELD, NORWEGIAN SEA.

3.1. Introduction.

In the first two chapters, we have presented the empirical and seismic methodologies used to calculate RPDTs. In this chapter, we will apply them to calculate RPDTs for Njord field, Norwegian Sea area. Our main purpose is to combine seismic RDPTs calculated from stacking velocity and empirical RPDTs to analyze rock physic properties in areas without well log information.

The workflow and main purposes of this chapter can be summarized as follows:

- ✓ Interpret well log and seismic data in Njord field to understand which factors are significant during the modeling of RPDTs.
- ✓ At well locations, model empirical RPDTs for normal mechanical compaction effect. Combine modelled depth trends and well log data to calculate so-called difference attribute depth trends. Interpret possible unexpected rock physic events that have occurred during burial history.
- ✓ Model RPDTs for unexpected rock physics events. Optimal rock physic properties could be obtained by fitting the modelled depth trends to well log data.
- ✓ Calculate interval velocity and other RPDTs from final stacking velocity. We expect that if the stacking velocity has good quality, the seismic interval velocity calculated by DIX equation will match nicely to sonic logging data. This means that we can replace well velocity by seismic interval velocity to interpret rock physics events and to quantify their properties in the area without well data.
- ✓ Calculate seismic interval velocity and other RPDTs for locations away from the wells. Combine empirical and seismic RPDTs to interpret rock physic scenarios and to quantify rock physic properties.

3.2. Njord field data.

Njord field is located in the Norwegian Sea, offshore Norway, and is operated by Norsk Hydro. Njord field was discovered to have commercial oil and gas. The reservoir targets are

beneath the regional unconformity at base of Cretaceous. The base map of Njord field is in Figure 8.

Given data from Njord field include 3D seismic data, 3D final stacking Vp velocity and logging data. We will have quick interpretation of given data to understand the general tectonic activities, subsurface structure, lithology and diagenetic events, which could affect the modelling of empirical and seismic RPDTs.

The complexity of the geological structure influences the quality of the stacking velocity analysis. If the geological structure is simple with relative flat and horizontal layers, it is expected to have good interval velocity calculated from stacking velocity by using the DIX equation. Otherwise, advanced methods in Table 1 are more appropriate to calculate interval velocity.

Seismic data and interpretation of local geology

Qualitative seismic interpretation helps us to understand the regional tectonic activities and stratigraphy sequences in Njord field.

Seismic inline 1787 is displayed in Figure 9. This inline goes through well 6407/7-1S showing the structure from 2 km downwards. A nearby seismic inline 1769 in Figure 10 shows the structure at shallow depths.

In term of complexity of geological structures and tectonic activities, we can divide the stratigraphy into two parts above and below Cretaceous unconformity.

The complex structure below Base Cretaceous contains tilted fault blocks where pre-rift and syn-rift sedimentary rocks can be found. Rifting phase terminated by the end of Jurassic. Tilting and erosion of the structure highs occurred during rifting and created an unconformity at the base of Cretaceous.

Above the unconformity, the structure was formed in a relatively stable tectonic environment. It contains relatively horizontal and flat layers. Regional subsidence is the dominant activity. Post rifting sediment has thick layers in both flanks of structure highs. Clay and mudstone are interpreted as dominant rocks in subsiding system.

Stacking velocity data.

The quality of final stacking velocity decides the quality of calculated interval velocity. By examining migrated seismic sections we see that the stacking velocity has functioned very

well in terms of fault-structure discrimination and multiple-diffraction attenuation. This encourages us to use stacking velocity to calculate interval velocity depth trend.

A display of final stacking velocity at well location 6407-7-1S is shown in Figure 11. Each velocity-analyzed point has one pair of velocity (rms) and two way traveltime (TWT). These values are used as inputs to calculate interval velocity.

Well log data.

The information about lithology is very important to analyze empirical RPDTs. Cutting description report in well 6407/7-1 is summarized in Table 3. In general, lithologies from the top of section down to the base of Cretaceous change gradually from clay to claystone. Below this depth, there are sandstone layers interbedded with siltstones.

Depth (m)	Cutting Description.
353-480	Unconsolidated sand with minor silt and clay.
480-1090	Clay with minor sand and silt throughout.
1090-1655	Claystone with minor stringers of siltstone. Olive green to light to medium green/grey/brown. Hardness varies from soft to firm. There is a gradational change from clay to claystone between 1090m and 1170m. Between 1410m-1510m, siltstone becomes evident.
1655-1975	Claystone with occasional very thin stringers of limestone and dolomite.
1975-2695	Claystone dominates with intermittent sandstone stringers to 2450m. Medium grey to grey/black, brown/grey and dard red/brown. Hardness varies from firm to moderately hard. Below 2450m, thicker sandstone and dolomite stringers become more common. Sandstone dominants claystone.
2695-3184	Series of interbedded sandstones and siltstones, which form the reservoir. Top of section has 5m limestone.
3184-3950	Inter-bedded sandstone and claystone.

Table 3: Cutting description in well 6407/7-1.

Logging data of density (RHOB), Gama ray (GR) and velocity (Vp and Vs) are available in wells 6407/7-1S and 6407/7-3. Porosity is calculated from density log using equation (11) assuming that claystone is dominant. The availability of shear wave velocity in

well 6407/7-3 throughout the reservoir section is useful for evaluating the modelled Vs depth trends. Displays of log curves for each well are shown in Figure 12 and 13, respectively.

We have evaluated the given data in Njord field. A summary of key interpretation points, which are critical for the RPDT modelling, is listed below:

- ✓ Structure above base of Cretaceous is simple with relative flat and horizontal layers. It is reasonable to apply DIX equation to calculate interval velocity from stacking velocity. Below this depth, the geological structure is complicated; DIX conversion method has limitation to handle dipping events and lateral variations in velocity so that other advanced methods in Table 1 may be preferable.
- ✓ From seabed down to 1.1 (km), it is possible to have early calcite cementation in sandstone stringers. From 1.1 (km) to 1.94 (km), the porosity is abnormally high. It may indicate that there is another diagenetic event beside normal mechanical compaction that has prevented water escape from clay materials and preserved high porosity.
- ✓ Uplifting and erosion at base of Cretaceous should be included to empirical RPDTs modelling. Study about the tertiary uplift and erosion along the Norwegian margin by Sven Hansen (Hydro Research Centre, 2001) showed that, at well 6407/7-1S, the uplifted thickness varies from 200 to 500 (m). It is noted that at flanks of structure highs, it is difficult to recognize discontinuities in sediments. Erosion may have not occurred in some parts of the area.
- ✓ Below base of Cretaceous, there is indication of late cementation, where the porosity is close to 0 and the velocity is very high. In the deeper part, when the formation is over consolidated, empirical normal mechanical compaction RPDTs will not be applicable.

3.3. Calculation of empirical rock physics depth trends.

First of all, we model empirical RPDTs in Njord field for normal mechanical compaction effect. The results will then be compared to well log data to interpret other possible unexpected rock physic events may have occurred during burial. Hereinafter, we consider unexpected events, which are different from normal mechanical compaction as *abnormal rock physic events*. If there is any abnormal rock physic event, it should be included

into modelling to obtain more realistic empirical RPDTs. By fitting the empirical RPDTs to the well log data, we can estimate rock properties of the abnormal rock physic events.

Empirical RPDTs are modelled for predefined lithologies that exist in sub surface. Avseth et al. (2005) suggested the common lithologies in silisiclastic environtments as in Table 3. The values listed in this table can be modified to match the real rock in the studying area.

Lithology	Initial porosity (A)	Clay sensitivity factor (β)	Framework grain stability factor (α)	Clay index (CI)	Density [kg/m^3]
Clean sand (SST)	0.40	0.27	0.1	0.1	2650
Shaly sand (SHY)	0.30	0.27	0.1	1.5	2660
Mud stone (MUD)	0.70	0.23	0.4	3.0	2680

Table 3: Parameters used to calculate porosity depth trends for different lithologies.

To model empirical RPDTs for a particular lithology at a certain depth, we assume that the overburden contains the same type of lithology.

Based on cutting descriptions, we consider the main lithology in overburden to be mudstone. We will model empirical RPDTs for the predefined lithologies in Table 3. We will also show how we can guide the modeling of RPDTs by predefined litho stratigraphic intervals.

As discussed in the theory part, the modelling of empirical RDPTs for either a mechanical compacted formation or other rock physic scenarios implies the following workflow:

- ✓ Model porosity depth trend.
- ✓ Calculate dry and saturated rock moduli depth trend.
- ✓ Calculate Vp and Vs depth trends.

- ✓ Calculate other RPDTs of Vp/Vs ratio, acoustic impedance.

These steps are programmed in MATLAB and combined into CLARA software (Ref: Flesche and Avseth, 2002, in-house software, Norsk Hydro) for further uses. The important program codes are included in the Appendix A.

3.2.1. Modelling and interpretation of normal mechanical compaction RPDTs.

Modelling of normal mechanical RPDTs.

Porosity depth trends of different predefined lithologies are calculated by equation 10. The parameters used in equation 10 are defined in the Table 3.

In order to calculate rock moduli at a certain depth, we need to calculate the density, effective pressure and coordination number. Overburden density can be calculated by summing cumulatively the average bulk density from seabed to the current depth. To calculate effective pressure, we assume that the overburden lithology contains mainly clay and formation fluid is brine water (this assumption is appropriate for this area). Equation 22 is used to calculate effective pressure. The coordinate number is calculated directly from porosity using equation 23.

We use Hert-Mindlin theory to calculate dry rock moduli and Gassmann theory to calculate saturated rock moduli.

Vp and Vs velocities are calculated by using equation 12 and 13. We can simply calculate Vp/Vs ratio and multiply density and velocity to get the acoustic impedance.

Modelled empirical RPDTs for different predefined lithologies under effect of mechanical compaction at well location 6407/7-1S are shown in Figure 14. They are displayed together with well log data for comparisons in Figue 15.

Interpretation of normal mechanical compaction RPDTs.

In general, normal mechanical compaction RPDTs do not match very well to the well log data at well location 6407/7-1S. Following we will try to evaluate in detailed what caused the mismatches and suggest method to improve empirical RPDTs.

First of all, we generate the difference attribute trends by subtracting normal mechanical compaction trends from well log data as shown in Figure 16. These trends are useful to interpret the abnormal rock physic events. In the velocity difference depth trend, we consider

the positive deviation as indicator of cemented sand and the negative deviation as indicator of abnormal high porosities.

Important interpretation points are summarized below:

- ✓ From seabed to 1.1 km, formation contains clay with minor unconsolidated sandstone and silt. Measured porosity varies from 20% to 45%, averagely 30%. The measured porosity in this interval is much lower than expected for mudstone. Possibly, the lithology in well 6407/7-1S is complicated with more sandstone and siltstone. That causes porosity to be lower, whereas density and velocity are higher than expected for mudstone.
- ✓ From 1.1 to about 1.9 km, formation contains mainly claystone. There is siltstone and occasionally very thin stringers of limestone and dolomite. The log porosity is much higher than modelled porosity trend for mudstone. It suggests that this is an abnormal rock physic interval where burial processes have prevented clays from loosing brine water and the clays are under compacted with abnormally high porosities. Abnormally high porosities reduce bulk rock densities and lower velocities in this interval.
- ✓ From 1.9 to 2.7 km, claystone dominates the formation. In the deeper part, thick layers of sandstone become more evident. Claystone in this interval has properties different from the interval above in hardness, compaction, colours and maturity. Modelled RPDTs fit quite better to log data. However porosity depth trend is still lower than measured porosity. Probably, we can apply the same method to adjust porosity to have better matches in density and velocity.
- ✓ At base of Cretaceous (2.69 km), log data changes dramatically. We should include uplifting and erosion effect to empirical RPDTs.
- ✓ Below the base of Cretaceous, rock contains interbedded sandstone and claystone. Hence the modelled velocity trends are too low compared to sonic log. It probably reflects presence of late cementation in this interval.

In summary, there are three main reasons for the mismatches between modelled RPDTs and well log data. First, the real lithologies are different with the predefined lithologies in Table 3. Second, the assumption ‘overburden has the same type of lithology’ has been violated due to the different lithologies in overburden. And third, there are other digenetic

events (abnormal rock physic events) occurred together with normal mechanical compaction that we have not included into the modelling.

To avoid the first two problems, we suggest to divide the stratigraphy into 4 intervals as in Figure 10 and then define the related rock parameters for empirical RPDTs modelling. And, to overcome the third problem, we should include abnormal rock physic events that have been revealed into the modelling.

We do not have enough well log data and laboratory measurements to define rock physic parameters for the intervals as suggested. They are left for future works. However we could improve the modelled empirical RPDTs in Njord field by including the following works:

- ✓ From 1.1-1.9 (km) adjust the modelled porosity for mudstone to match the measured porosity then recalculate density and velocity depth trends.
- ✓ At base of Cretaceous (2.69 km), include the uplift and erosion effect. The eroded thickness varies from 200-500 (m).
- ✓ Below 2.69 (m), model empirical RPDTs with the effect of late cementation effect.

3.2.2. Modelling of empirical RPDTs for abnormal rock physic events.

In this part, we will model empirical RPDTs for abnormal rock physic events, which have been interpreted previously, together with normal mechanical compaction effect. Logging data in well 640777-1S are used for fitting to get the optimal parameters of abnormal rock physics events.

Modelling of cementation RPDTs.

Dvorkin theory is used to model empirical RPDTs for cementation effect in sandstone intervals. Because there is little or no cementation in mudstone, its modelled RPDTs are kept unchanged.

To model RPDTs, we need to define critical porosity before the first cement initiates. This value can be determined by analyzing porosity in a clean sand interval above the cemented section. To simplify, we assume the critical porosity is 0.1-1% higher than the porosity when the first cement initiated.

In the cemented sandstone interval, the porosity reduces with depth. We assume that the decrease in the porosity is caused mainly by cementation. In another words, we can calculate the cement volume by subtracting the porosity depth trend values from the critical porosity.

Modelling of abnormal porosity RPDTs.

In the abnormal high porosity intervals, we will adjust the porosity depth trends to the porosity log curve and recalculate other RPDTs. As we can see in Figure 15, porosities do not follow the porosity trend modelled for normal mechanical compaction effect. To simplify, we assume the porosity decreases linearly. By adjusting to porosity log curve we can define the low end and high end of porosity in the abnormal porosity intervals. RPDTs of density and velcocity are calculated accordingly.

Modelling of uplifting-erosion RPDTs.

Base of Cretaceous is found at 2.695 (km). The eroded thickness varies from 200-500 (m). We treat the effect of uplifting and erosion as a discontinuous mechanical compaction mechanism to model empirical RPDTs.

Introduction to CLARA software.

CLARA is a MATLAB software programmed by Harald Flesche and Per Avseth (Norsk Hydro Research Centre, 2002). This software is used to calculate normal mechanical compaction RPDTs and apply them for AVO analysis.

In this study, we have modified the original version to include other abnormal rock physics events together with normal mechanical compaction effect for modelling of empirical RPDTs.

The interface of CLARA software and MATLAB codes are presented in the Appendix C.

Results and discussions.

The results of empirical RPDTs modelled for all abnormal rock physics events are shown in Figure 17. The same results compared with well data are shown in Figure 18.

As we can see, new RPDTs fit much better to well data in clay and claystone section above base of Cretaceous and in the below sandstone/siltstone section. It proves that the interpretation about the abnormal rock physics events is reliable. We can use the RPDTs of mudstone above base of Cretaceous and RPDTs of sandstone below base of Cretaceous as

general trends in the structure high in Njord field for further rock physic analysis such as AVO analysis.

In order to model successfully the RPDTs for abnormal rock physics events, we desire to quantify the following parameters:

Abnormal high porosity/Overpressure in claystone.	***Uplifting-Erosion***	***Cementation***
Depth interval	Depth interval	Depth interval
Porosity function	Eroded thickness	Cement volume

Table 4: Abnormal rock physics events properties need to be quantified.

Information about the depths where the abnormal rock physic events initiate and end can be estimated by evaluating the difference attribute depth trends in Figure 16. Correlation between seismic horizons and well data is another useful source to obtain this information.

It is possible to find other parameters by fitting the modelled RPDTs to well log data. We have fitted the porosity trend to the porosity log curve to obtain the optimal porosity function. In the area without well data, we can obtain porosity function by adjusting porosity until the modelled velocity trend fit nicely to the seismic interval velocity. We can use the same fitting method to obtain the optimal eroded thickness.

It is difficult to determine accurately the volume of cement in cemented sandstone interval. We assume that the reducing porosity in cemented sandstone interval is equal to the cement volume. This assumption is quite reasonable in small sandstone intervals but not in thick sections contain different type of lithologies. The estimated cement volume is normally higher than reality.

In the interval from 1.1 to 1.9 (km), where we observed an abnormally low velocity depth trend, we may interpret this interval as an overpressure interval. As we know, overpressure reduces the Vp velocity. However, when we assume normal hydrostatic pore pressure and increase the porosity depth trend to match logging porosity data to recalculate the RPDTs, the velocity depth trend fits very well to sonic velocity. It implies the likelihood that the overpressure occurred during shallow burial for a period of time then was released to be normal. High porosities have been preserved during and after overpressure.

Since we do not know the detailed litho stratigraphy at the well location, it caused us difficulties in choosing optimal RPDTs for quantification of rock physic properties. It would be better if we were able to divide lithology column into several intervals and define their properties as in Table 3.

To summarize, we suggest the following workflow to interpret and quantify the rock physic events at well locations in Njord field:

- ✓ Step 1: Combining the qualitative seismic interpretation with logging data to define rock intervals where the lithology and rock physic properties are similar. For example in Njord field we can define four different intervals as in Figure 10.
- ✓ Step 2: Using well log data and laboratory data to define the rock properties in each rock interval for empirical RPDTs. Especially, define the parameters in equation 10 to calculate porosity depth trend using Ramm and Bjørlykke theory.
- ✓ Step 3: For a particular rock interval at well locations, calculate the normal mechanical compaction RPDTs for defined lithologies. Generate the difference attribute trends to interpret the abnormal rock physics events.
- ✓ Step 4: Modelling RPDTs for the effect of abnormal rock physics events together with normal mechanical compaction. Fitting the modelled depth trends to well log data to quantify the properties of abnormal rock physic events as listed in the Table 4.

Away from well locations, we will use seismic RPDTs to interpret rock physic events and quantify their rock physic properties. This is presented in the next section.

3.4. Calculation of seismic rock physics depth trends.

We follow the procedures in chart 1 to calculate seismic RPDTs for Njord field. The work is programmed in MATLAB and important program codes are included in Appendix B.

Interval compressional velocity (Vp) calculation.

The workflow can be summarized:

- ✓ Read rms data {TWT [ms], velocity [m/s]} for desired locations {Inline, Xline}.
- ✓ Calculate interval velocity using equation (2).
- ✓ Convert interval traveltime to depth.
- ✓ Display interval velocity in depth domain.

A display of stacking velocity data versus TWT for inline 1788 is in Figure 19. In this plot, we can observe the velocity picks at different crosslines. Crossline increment is 20, from 450 to 1350.

Interval velocity for each interval is calculated by using DIX equation. The interval thickness is calculated by multiplying interval velocity with the oneway traveltime. We can add interval thicknesses together to obtain total thickness. The calculated seismic interval velocities are plotted versus depths in Figure 20. The stair curve is the interval velocity at well location 6407/7-1S.

Other rock physics depth trends calculation.

In order to calculate Vs depth trend we have to use empirical relations. Shear velocity Vs (km/s) is calculated by using equation (9) proposed by Castagna et al. (1985, 1993), $V_S = 0.8042V_P - 0.8559$. Calculated Vs and Vp at well location 6407/7-1S are plotted in Figure 21.

Density is calculated by using Castagna equation (13) and porosity is calculated by using equation (11) for different lithologies of sandstone, shale and mudstone.

Results and discussions.

Seismic RPDTs are modelled and compared to logging data at well location 6407/7-1S. The results are shown in Figure 22. We observe a good match between seismic velocity and sonic velocity, especially in the section above base of Cretaceous. Just below this depth, there is an abrupt change in velocity. As described in lithology column, there is 5m limestone below base of Cretaceous. Probably, high velocity in limestone and the unconformity affected the stacking velocity analysis and caused this high pick. At greater depths, the interval velocities match reasonably to the well log data.

In Figure 23, interval velocities are calculated for the entire inline 1788 and plotted together with well log data. Above base of Cretaceous, the interval velocities are consistent between different locations. However below this depth, the interval velocities are dispersive. There are several too high and too low velocity picks indicating the stacking velocities were mis-picked on the multiples or diffractions. The sensitivity of stacking velocity with depth could be another reason, where different velocities may result in the same quality of a stacked section.

The density and porosity depth trends calculated for mudstone match pretty well to log data except in the interval from about 2.0-2.7 (km). Probably, Castagna equations are not suitable to apply for lithologies in this interval.

In summary, we conclude that, above base of Cretaceous, interval velocity converted from stacking velocity by using DIX equation has good quality. We can use the seismic interval velocity instead of well log velocity in the areas away from well locations for rock physic analysis. Below base of Cretaceous, the interval velocity does not match very well to sonic velocity data. We suggest to re-pick the stacking velocities to get better quality and also to use more advanced method to calculate the interval velocity as in the Table1.

Continuing the results and discussion in section 3.2.2, to interpret rock physic events and quantify their rock properties in new areas away from well locations, we suggest:

- ✓ Step 5: Using the structural seismic interpretation results to correlate and define the rock intervals at current location based on the defined intervals at well locations in step 1.
- ✓ Step 6: Using the predefined parameters in step 2 to calculate the normal mechanical compaction RPDTs.
- ✓ Step 7: Calculate the seismic interval velocity from stacking velocity using DIX equation. We can apply Castagna relations or establish new relations for Njord area to calculate density and porosity trends from velocity.
- ✓ Step 8: Calculate difference attribute depth trends between seismic RPDTs and normal mechanical compaction RPDTs to interpret unexpected/abnormal rock physic events.
- ✓ Step 9: Model the empirical RPDTs for all possible abnormal rock physic events. Fit the modelled depth trends to seismic depth trends to quantify rock physic properties. We can use the difference attribute depth trends calculated at well location from seismic and well log data to evaluate the uncertainty of quantified parameters.

3.5. Rock physic analysis in areas away from well locations.

In this part, we use seismic interval velocity to analyze the rock properties in areas away from well locations. We follow the workflow mentioned in section 3.4.

Seismic location at inline 2502 and crossline 910 is selected for this study purpose. Seismic section of inline 2549 is displayed in Figure 24 for reference.

Results and discussions.

Following, we will present the results for each steps suggested in section 3.4.

- ✓ Step 5: By correlating the seismic events to well location, we divide the lithology column into four intervals as in Figure 24. Due to limit of time and lack of data, we were not able to define lithology properties for each interval as suggested. For the time being, we stay with modelling empirical RPDTs for predefined lithologies in Table 3.
- ✓ Step 6: Normal mechanical compaction RDPTs are displayed in Figure14.
- ✓ Step 7: The results of seismic RPDTs are in Figure 25. For comparison, velocity in selected location is plotted together with the calculated interval velocity for the whole inline 2502. The interval velocities are consistent down to 3 (km). Below this depth, velocity picks are dispersive. We have used the Castagna transform equations to calculate density for sandstone and shale. We do not have empirical relation to calculate density for mudstone. Porosity depth trends are calculated for sandstone and shale from density trends using equation 11.
- ✓ Step 8: The difference attribute trends calculated from seismic interval velocity at the current location are displayed in Figure 26. For comparison, the difference attribute trends calculated from seismic interval velocity at well location 6407/7-1S are shown in Figure 27. We observe the same characteristics in the difference velocity trends. We conclude that there are unexpected rock physic events occurring besides normal mechanical compaction at the current location. These events have similar characteristics with those occurred at the well location 6407/7-1S.
- ✓ Step 9: Final empirical RPDTs modelled for all possible rock physic scenarios by fitting to seismic interval velocity are shown in Figure 28. Mudstone as defined in Table 3, is used for quantifying rock physics parameters in the abnormal high porosity interval.

In summary, we can combine seismic RPDTs and empirical RPDTs to interpret and quantify rock physic properties for normal mechanical compaction effect and other unexpected rock physic events. In areas without well information, the seismic interval velocity trend is useful for rock physic analysis, especially for overburden. The RPDTs can furthermore be used to constrain AVO analysis, but this is beyond the scope of this study.

CONCLUSIONS

- ✓ We have developed the methodologies to model empirical and seismic rock physic depth trends (RPDTs).
- ✓ Normal mechanical compaction RPDTs are modeled for predefined lithologies. We can combine well log data with normal mechanical compaction RPDTs to interpret unexpected rock physic events such as cementation, uplifting-erosion and overpressure.
- ✓ If there are unexpected rock physic events occurring besides normal mechanical compaction, they should be included into the modeling step to have better empirical RPDTs. To quantify the properties of unexpected rock physic events, we suggest using the workflow in section 3.2.2 (step 1 to step 4).
- ✓ Seismic interval velocity can be calculated from stacking velocity using DIX equation. This method is highly applicable in the simple geological structures where sediments have deposited in relatively horizontal and flat layers. In complicated geological structures, other advanced methods in Table 1 are preferable to calculate interval velocity.
- ✓ In area without well log information, we can combine seismic and empirical RPDTs to interpret the rock physic scenarios and quantify unexpected rock physic event. The workflow is suggested in section 3.4 (step 5 to step 9).
- ✓ We have conducted a case study for Njord field, Norwegian Sea area. The seismic interval velocity matches nicely to well log data, especially above base Cretaceous where the structure is simple with flat and relative horizontal layers. Below base Cretaceous, we suggest to reprocess the stacking velocity to include the effects of the uplifting-erosion and late cementation to get higher velocity in this interval. Other advanced methods to calculate interval velocity for complex geological structures may be preferable.
- ✓ We suggest using seismic interval velocity depth trend above base Cretaceous for further AVO depth trend calculation.
- ✓ We were successful in modeling empirical RPDTs for normal mechanical compaction for predefined lithologies in Table 3. We can use logging data at well locations or

seismic RPDTs in areas without well log information to interpret and quantify properties of rock physic events.

- ✓ Beside normal mechanical compaction, overpressure, uplifting-erosion and late cementation events have occurred in Njord field. During fitting modelled RDPTs to well log data we found that overpressure had occurred from 1.1 to 1.9 (km). Overpressure had prevented rock from mechanical compaction and preserved high porosity. After sometime, high pressure was released to be normal but the porosity still remained abnormally high. High porosity causes low velocity in this interval.
- ✓ Since we do not have enough information about the lithology column, we were not able to quantify reliably the properties of unexpected rock physic events in areas away from well locations. For future works, we can improve this step by following the suggested workflow in section 3.4.

ACKNOWLEDGEMENTS

First of all, I would like to express my sincere thanks to NORAD fellowship program for giving me a great opportunity to come and study in the Norwegian University of Science and Technology (NTNU), in Trondheim, Norway.

I had permission to conduct my thesis in the Research Centre of Norsk Hydro in Bergen. During my stay, Hydro has kindly supported me accommodation, computer and free accesses to data. I acknowledge people in the Seismic Analysis Group for their valuable advises and helps.

My thesis has been done under the supervision of Professor Bjørn Ursin (NTNU) and Doctor Per Avseth (Norsk Hydro). I admire their professional knowledge and appreciate them for guiding me through every step of this project.

I would like to thank professors and staffs in the Petroleum Engineering and Applied Geophysics department, especially to Egil Tjåland, Alexey Stovas and Tone Sanne. Thank you for teaching and helping me during my study in our department.

Finally, I would like to send many thanks to my dear family back home and friends who have been continuously encouraging and supporting me in the last two years. Special thanks to T.Q Nghia and H. Anh. Their warm friendship keeps me awake throughout the frozen winter in Trondheim.

Tusen takk**.**

REFERENCES

1. Avseth, P., Mekerji T., Markov G., 2005. *Quantitative Seismic Interpretation*. Cambridge University Press.
2. Avseth, P. and Bachrach, R. 2002. *Seismic properties of consolidated sands: Tangential stiffness, Vp/Vs ratios and diagenesis*. E&P Research Centre Bergen, Norsk Hydro.
3. Carcione, J. M. and Helle, H. B., 2002. *Rock physics of geopressure and prediction of abnormal pore fluid pressure using seismic data*. E&P Research Centre Bergen, Norsk Hydro.
4. Carcione, J. M., Helle, H. B., Pham, N. H. and Tovrud, T., 2001. *Pore pressure estimation from seismic reflection data*. E&P Research Centre Bergen, Norsk Hydro.
5. Dvorkin, J., Nur, A., and Yin, H., 1994. *Effective properties of cemented granular material*. Mech. Mater., 18, 351-366.
6. Hansen, S., 2001. *Tertiary uplift and erosion along the Norwegian Margin*. E&P Research Centre Bergen, Norsk Hydro.
7. Hilterman, F. J., 2001. *Seismic amplitude Interpretation*. Distinguished Instructor Series, No.4.
8. Hashin, Z., and Shtrikman, S., 1963. *A variational approach to the elastic behaviour of multiphase materials*. J. Mech. Phys. Solids, 11, 127-140.
9. Brevik, I., 2005. *Burial processes and their control on acoustic properties in shales*. Statoil R&D Centre.
10. Mindlin, R. D., 1949. *Compliace of elastic bodies in contact*. J. Appl. Mech., 16, 259-268.
11. Ramm, M., and Bjørlykke, K., 1994. *Porosity depth trends in reservoir sandstones: assessing the quantitative effects of varying pore-pressure, temperature history and mineralogy, Norwegian Shelf data*. Clay Miner., 29, 475-490.
12. Storvoll, V. and Bjørlykke, K., 2004. *Sonic velocity and grain contact properties in reservoir sandstones*. Petroleum Geoscience, Vol.10, pp.215-226.
13. Thomsen, L., 2002. *Understanding seismic anisotropy in exploration and exploitation*. Distinguished Instructor Series, No.5.
14. Ursin, B. and Stovas, A., 2005b, *Traveltime approximation for layered transversely isotropic medium,* Geophysics, accepted for publication.
15. Ursin, B. and Stovas, A., 2005a, *Generalized Dix equation for a layered transversely isotropic medium,* Geophysics, 70, N6, P.D77-D81.
16. Worden, R.H. and Burley, S.D., 2003. *Sandstone diagenesis: The evolution of sand to stone*.
17. Yilmaz, O., 2002, *Seismic data analysis*. Investigations in Geophysics 10, Vol. 2.

APPENDIX

A. MATLAB codes to calculate empirical RPDTs.

A.1 Calculation of empirical RPDTs.

```
function depth_model(cmd)
% calculate depth trends, do fluid substitution, plot depth trends
for all lithologies and pore fluids make possibility for import of
log data for calibration.

if nargin == 0
    cmd = 'init';
end

switch cmd
case {'init','view'}


main_f=findobj('tag','avo_class');
model = get(main_f,'userdata');
z = (model.rp.waterdep:0.01:model.rp.maxdep)';
z_bur = z-model.rp.waterdep;

% Read userdata to see if there are diagenetic events.

      cd1=model.dia.cd1;    cd2=model.dia.cd2;  cd3=model.dia.cd3;
      cd4=model.dia.cd4;    ud=model.dia.ud;     et=model.dia.et;
      ap1=model.dia.op1;    ap2=model.dia.op2;

    if (cd1 >0) & (cd2> cd1)
        cm1='Y';
        icm1 = int32(interp1(z,1:1:size(z,1),cd1));
        icm2 = int32(interp1(z,1:1:size(z,1),cd2));
    else cm1='N'
    end

    if (cd3 >0) & (cd4> cd3) & (cd3 > cd2)
        cm2='Y';
        icm3 = int32(interp1(z,1:1:size(z,1),cd3));
        icm4 = int32(interp1(z,1:1:size(z,1),cd4));
    else cm2='N'
    end

    if (ud>0) & (et>0)
        ue= 'Y';
        iue1 = int32(interp1(z,1:1:size(z,1),ud));
    else ue='N'
    end

    if (ap1>0) & (ap2>ap1)
        AP1='Y'
        iap1=int32(interp1(z,1:1:size(z,1),ap1));
        iap2=int32(interp1(z,1:1:size(z,1),ap2));
    else AP1='N'
    end
```

```
% Assume having only mechanical compaction
por =   repmat(model.rp.por,size(z,1),1).*…
        exp(z_bur*(model.rp.frame+model.rp.sens.*model.rp.CI)) ;

[rho,p_eff,n]=parm(model,z,por);
[K_dry,Mu_dry]=Compaction(n,p_eff,rho,por,model,z);

%------------------
% If there is over pressure.
if AP1=='Y'
por_ap1=0.47;
por_ap2=0.32;
p_eff_dec=0

litho=3
int3=iap1:iap2
num1=size(int3,2)
num2=por_ap1-por_ap2
num3=num2/num1
por(iap1,litho)=por_ap1
for i=iap1+1:iap2;
    por(i,litho)= por(i-1,litho)- num3;
end


[rho_tmp,p_eff_tmp,n_tmp]=parm(model,z,por);
rho(int3,litho)=rho_tmp(int3,litho);

p_eff(int3,:)= p_eff(int3,:)-p_eff_dec.*p_eff(int3,:);
[K_dry,Mu_dry]=Compaction(n,p_eff,rho,por,model,z);
end

%-------------
% If there is uplifting and erosion.

[K_sat,Mu_sat,rho_sat] = satmoduli(K_dry,Mu_dry, por, model,z);
[Vp_sat,Vs_sat] = vel(K_sat, Mu_sat, rho_sat);

inc=round(et/0.01);
max1=size(z,1);

if ue=='Y'
    zue=(model.rp.waterdep:0.01:(model.rp.maxdep+et+0.01))';
    [por_ue,rho_ue,p_eff_ue,n_ue]=parm2(model,zue);
    size(por_ue);

    i1=iue1+inc;
    i2=max1+inc;

    por(iue1:max1,:)= por_ue(i1:i2,:);
    rho(iue1:max1,:)=rho_ue(i1:i2,:);
    p_eff(iue1:max1,:) = p_eff_ue(i1:i2,:);
    n(iue1:max1,:) = n_ue(i1:i2,:);
end

[K_dry,Mu_dry]=Compaction(n,p_eff,rho,por,model,z);
[K_sat,Mu_sat,rho_sat] = satmoduli(K_dry,Mu_dry, por, model,z);
[Vp_sat,Vs_sat] = vel(K_sat, Mu_sat, rho_sat);
```

```
% If there is cementation

if cm1=='Y'
    int1=icm1:icm2;

    tmp=[K_dry(int1,3), Mu_dry(int1,3)];
    zc=z(int1);
    nc=n(icm1,:);
    porc=por(int1,:);
    porc_c=por(icm1,:);


    [K_dry(int1,:);
    Mu_dry(int1,:)]=Cementation(nc,porc,porc_c,model,zc);

    K_dry(int1,3)=tmp(:,1);  Mu_dry(int1,3) = tmp(:,2);
    tmp=[Vp_sat(int1,3),Vs_sat(int1,3)];

    [K_sat(int1,:),Mu_sat(int1,:),rho_sat(int1,:)] =
    satmoduli(K_dry(int1,:),Mu_dry(int1,:), porc, model,zc);

    [Vp_sat(int1,:),Vs_sat(int1,:)] = vel(K_sat(int1,:),
    Mu_sat(int1,:), rho_sat(int1,:));

    Vp_sat(int1,3)=tmp(:,1); Vs_sat(int1,3) = tmp(:,2);
end


if cm2=='Y'
    int2=icm3:icm4;
    tmp1=[K_dry(int2,3), Mu_dry(int2,3)];
    tmp2=[K_dry(int2,2), Mu_dry(int2,2)]
    zc=z(int2);
    nc=n(icm3,:);
    porc=por(int2,:);
    porc_c=por(icm3,:)+0.03;
    por(int2,1:2)=porc(:,1:2);

    [K_dry(int2,:),
    Mu_dry(int2,:)]=Cementation(nc,porc,porc_c,model,zc);

    K_dry(int2,3)=tmp1(:,1);
    Mu_dry(int2,3) = tmp1(:,2);
    K_dry(int2,2)=tmp2(:,1);  Mu_dry(int2,2) = tmp2(:,2);
    tmp1=[Vp_sat(int2,3),Vs_sat(int2,3)];
    tmp2=[Vp_sat(int2,2),Vs_sat(int2,2)];


    [K_sat(int2,:),Mu_sat(int2,:),rho_sat(int2,:)] =
    satmoduli(K_dry(int2,:),Mu_dry(int2,:), porc, model,zc);

    [Vp_sat(int2,:),Vs_sat(int2,:)] = vel(K_sat(int2,:),
    Mu_sat(int2,:), rho_sat(int2,:));

    Vp_sat(int2,3)=tmp1(:,1); Vs_sat(int2,3) = tmp1(:,2);
    Vp_sat(int2,2)=tmp2(:,1); Vs_sat(int2,2) = tmp2(:,2);
end
```

```
% Save all calculated values into a structure
    d_model.z = z;
    d_model.por = por;
    d_model.rho = rho;
    d_model.peff = p_eff;
    d_model.n = n;
    d_model.K_dry = K_dry;
    d_model.Mu_dry = Mu_dry;
    d_model.K_sat = K_sat;
    d_model.Mu_sat = Mu_sat;
    d_model.rho_sat = rho_sat;
    d_model.Vp_sat = Vp_sat;
    d_model.Vs_sat = Vs_sat;

% Save calculated parameters to a userdata
model.d_model=d_model;
set(main_f,'userdata',model)
```

A.2 Related functions.

```
function [K_d, Mu_d]=Cementation(n,porc,por_c,model,zc)
       % Function to calculate dry rock moduli in case of cementation
       using Dvokin theory.


        % Ussume that cement is Quartz
        K_c = 36.8e9;
        Mu_c = 44e9;
        % Mineral rock moduli from initial model
        K_s = repmat(model.rp.k,size(zc,1),1);
        Mu_s = repmat(model.rp.mu,size(zc,1),1);

        % Initial porosity for different lithology
        por_c = repmat(por_c,size(zc,1),1);
        n = repmat(n,size(zc,1),1);

        vc = 0.5*(K_c/Mu_c-2/3)/(K_c/Mu_c+1/3);
        vs = 0.5*(K_s./Mu_s-2/3)./(K_s./Mu_s+1/3);

        alpha = ((2/3)*(por_c-porc)./(1-por_c)).^0.5;
        Dn = 2*Mu_c.*(1-vs).*(1-vc)./(pi().*Mu_s.*(1-2*vc));
        Dt = Mu_c./(pi().*Mu_s);

        An = -0.024153*Dn.^(-1.3646);
        Bn = 0.20405*Dn.^(-0.89008);
        Cn = 0.00024649*Dn.^(-1.9864);

        At = -10^(-2)*(2.26.*vs.^2+2.07.*vs+2.3).*Dt.^
        (0.079.*vs.^2+0.1754*vs-1.342);

         Bt = (0.0573.*vs.^2+0.0937.*vs+0.202).*Dt.^
        (0.0274.*vs.^2+0.0529*vs-0.8765);
```

```
        Ct = 10^(-4).*(9.654*vs.^2+4.945.*vs+3.1).*Dt.^
        (0.01867.*vs.^2+0.4011.*vs-1.8186);

        Sn = An.*alpha.^2 + Bn.*alpha + Cn;
        St = At.*alpha.^2 + Bt.*alpha + Ct;

        M_c=K_c+4/3*Mu_c;

        K_d = n.*(1-por_c)*M_c.*Sn/6;
        Mu_d = 3*K_d/5 + 3*n.*(1-por_c)*Mu_c.*St/20;
    end


function [K_hm, Mu_hm]=Compaction(n,p_eff,rho,por,model,z)
        % Function to calculate dry rock moduli in case of mechanical
        % compaction only using Hert Mindlin theory:

        K_hm = ((n.^2.*(1-por).^2.*repmat(model.rp.mu,size(z,1),1)
        .^2.*p_eff)./18*pi^2.*(1-
        repmat(model.rp.poiss,size(z,1),1)).^2)) .^(1/3);

        Mu_hm = (5-4*repmat(model.rp.poiss,size(z,1),1))./(5*(2-
        repmat(model.rp.poiss,size(z,1),1))).*((3*n.^2.*(1-
        por).^2.*repmat(model.rp.mu,size(z,1),1).^2.*p_eff)./
        (2*pi^2*(1-repmat(model.rp.poiss,size(z,1),1)).^2)).^(1/3);

 end


function [por,rho,p_eff,n]=parm(model,z)
        % Function to calculate porosity, effective por, density and n

        % Overburden depth
        z_bur = z-model.rp.waterdep;

        % Porosity
        por = repmat(model.rp.por,size(z,1),1).*exp(-
        z_bur*(model.rp.frame+model.rp.sens.*model.rp.CI)) ;

        % Calculate the density for the different lithologies, given
        pore fluid BRINE
        rho = (1-por).*repmat(model.rp.rho,size(z,1),1)+
        por*model.rp.fl_rho(find(strcmp(model.rp.fluid,'BRINE')));

        % Assume overburden mainly clay, calculate effective pressure
        p_eff = repmat(cumsum(rho(:,find(strcmp(model.rp.lit,'MUD')))-
        model.rp.fl_rho(find(strcmp(model.rp.fluid,'BRINE'))))*9.8*10,
        1,3)

        % Calculate moduli according to Hertz-Mindlin contact theory
        % No. of concact points, 2nd order polynomial fit
                    n = 25.98805*por.^2-43.7622*por+21.6719;
end
```

B. MATLAB codes to calculate seismic RPDTs.

B.1 Calculation of seismic RPDTs.

```
%% Plot twt _ rms inline 596 and at well location 596-910
data1=load('well1S_rms_twt_IL596_XL910.txt');
x1=data1(:,2);
y1=data1(:,1);


data2=load('rmsvel_I596.txt');
x2=data2(:,2);
y2=data2(:,1);

figure1 = figure('PaperPosition',[0.6345 6.345 20.3
15.23],'PaperSize',[20.98 29.68]);

%% Create axes
axes1 = axes('XGrid','on','YDir','reverse','YGrid','on')
title(axes1,'Root Mean Squared Velocity Vs. Twoway Traveltime ,
Inline 1788');
xlabel(axes1,'RMS (m/s)');
ylabel(axes1,'TWT (ms)');
box(axes1,'on');
hold(axes1,'all');

%% Create plot
plot(x2,y2,'LineStyle','none','Marker','*');
hold on;
plot(x1,y1,'r','Marker','*')


%-------------------------------------------------------------------
fid3=fopen('d_intvel_I596.txt','w');
m=size(data2,1)/44;

for i =1:m

        TWT= data2(1+(i-1)*44:44+(i-1)*44,1);
        RMS= data2(1+(i-1)*44:44+(i-1)*44,2);
        [intvel,T,index]= DIX(TWT,RMS);
        intd = T(1:index).*intvel*0.5*10^-3;
        D=cumsum(intd(1:index)');
        Intv=intvel(1:index)';

        for j=1:index
        fprintf(fid3,'%12.4f %12.4f\n', D(j),Intv(j));
        end
end

data3=load('d_intvel_I596.txt');
x3=data3(:,2);
y3=data3(:,1);
data4=load('d_intvel_I596_X910.txt');
x4=data4(:,2);
y4=data4(:,1);
```

```
figure2 = figure('PaperPosition',[0.6345 6.345 20.3
15.23],'PaperSize',[20.98 29.68]);
%--------------------------------------------------------------------
% Ploting inteval velocity versus depth.

% Create axes
axes2 = axes( 'XGrid','on','YDir','reverse','YGrid','on')
title(axes2,'Interval Velocity vs. Depth, Inline 1788. ');
xlabel(axes2,'Interval velocity (m/s)');
ylabel(axes2,'Depth (m)');
box(axes2,'on');
hold(axes2,'all');

% Create plot
plot(x3,y3, 'LineStyle','none','Marker','*');
hold on;
stairs(x4,y4,'r');

%--------------------------------------------------------------------
% Ploting int_depth in well 1S, iline 1788-xline 910.

figure3 = figure('PaperPosition',[0.6345 6.345 20.3
15.23],'PaperSize',[20.98 29.68]);

% Create axes
axes1 = axes('XGrid','on','YDir','reverse','YGrid','on');
title(axes1,['Interval Velocity vs. Depth, ',char(10),'Well
location 6407-7-1S, Inline 1788, Xline 910    ']          );
xlabel(axes1,'Interval velocity (m/s)');
ylabel(axes1,'Depth (m)'); box(axes1,'on'); hold(axes1,'all');

% %% Create plot
plot4 = stairs(x4,y4); vs=(x4.*0.8042/1000-0.8559)*1000;
hold on
stairs(vs,y4,'r');
```

B.2 Related functions.

```
function [intvel, T, index]=DIX(TWT,RMS)
%Function to calculate interval velocity from TWT and RMS using
Dix eqt.

    T(1)=TWT(1)
    intvel(1)=RMS(1);
    for j =2:(size(TWT,1));
        if TWT(j) ~= TWT(j-1)
         intvel(j)=sqrt(abs((RMS(j).^2.*TWT(j)-RMS(j-1).^2.*TWT(j-
         1))  ./(TWT(j)-TWT(j-1))));

         T(j)=TWT(j)-TWT(j-1);
        end
    end
    index=min(find(TWT==max(TWT)));
end
```

C. Clara software.

C.1 Interface and main functions of CLARA software.

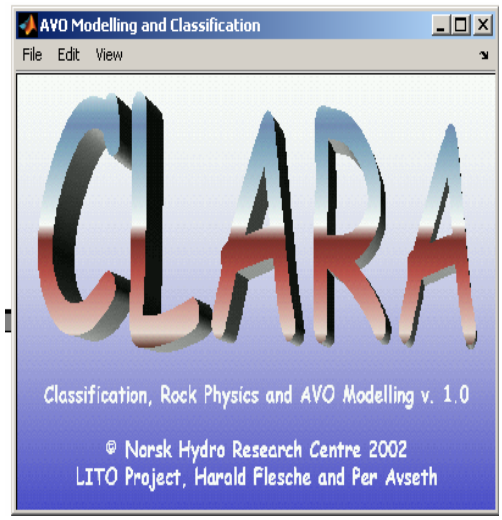

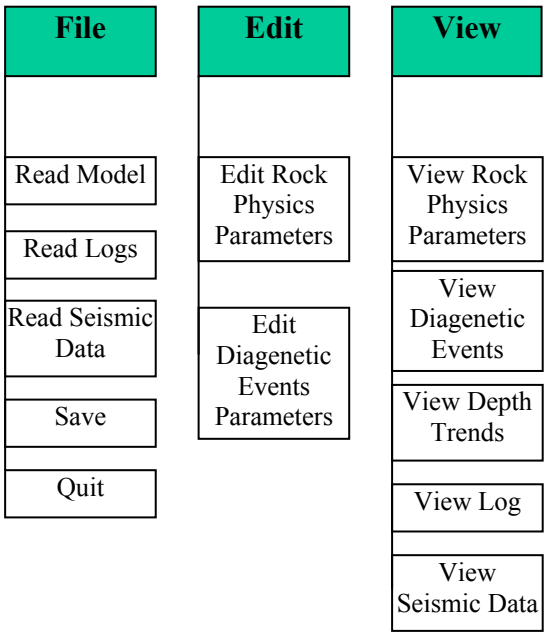

C.2 MATLAB codes.

Free access to MATLAB codes of CLARA software (modified version) is in the following address: *https://folk.ntnu.no/phuong/study/thesis*.

D. Figures.